Reduction in Coercive Force Caused by a Certain Type of Imperfection

A. AHARONI
Department of Electronics, The Weizmann Institute of Science, Rehovot, Israel
(Received February 1, 1960)

As a first approach to the study of the dependence of the coercive force on imperfections in materials which have high magnetocrystalline anisotropy, the following one-dimensional model is treated. A material which is infinite in all directions has an infinite slab of finite width in which the anisotropy is 0. The coercive force is calculated as a function of the slab width. It is found that for relatively small widths there is a considerable reduction in the coercive force with respect to perfect material, but reduction saturates rapidly so that it is never by more than a factor of 4.

I. INTRODUCTION

THE theory of micromagnetics[1] has been successful[2,3] in explaining the experimental measurements of magnetic properties of *small* ferromagnetic particles, or other cases in which the magnetocrystalline anisotropy energy is negligible. This theory, however, failed to agree with experiment[4] for particles large with respect to the characteristic radius $Ro=A^{\frac{1}{2}}/I_s$ of materials which have a relatively high magnetocrystalline anisotropy coefficient K.[4] In particular,[5] the theory did not yield any stable domain configuration, and the predicted coercive force was larger by orders of magnitude than the experimentally observed one.

Recently, DeBlois and Bean[6] have found experimentally that for the most perfect iron whiskers, a coercive force approaching the theoretical value could be obtained in certain *parts* of the samples. This experiment strongly suggests that the micromagnetic approach is fundamentally correct, but that the theory assumes materials too perfect and ideal to be realized experimentally. It seems therefore that the theory should be modified to include imperfections in order to fit the results in practical materials. The necessary modifications can in principle be one or more of the following types.

1. Finiteness

Up to now only an infinite circular cylinder was studied[7,8] rigorously. For finite bodies (sphere[5,9] and prolate ellipsoid[3]) only nucleation fields have been calculated, and it is not known theoretically what happens after nucleation. Now, while the whiskers in the DeBlois and Bean[6] experiment can be regarded as infinite cylinders when they are studied at some midpoints, they can be regarded at best as semi-infinite cylinders when studied near each end. It is therefore possible that the finiteness of the samples is responsible for the much lower coercive force near the ends of the whiskers. The theoretical study of some finite, or at least semi-finite bodies seems thus an essential part of the theory and will have to be undertaken in the future. It is, however, a rather complicated mathematical problem and will be ignored in this paper.

2. Surface Roughness

For the theoretical study of the infinite cylinder it is assumed that the surface is absolutely smooth, which is never the case in practical samples. The high demagnetizing field due to scratches and other irregularities of the surface might give rise to a local field large enough to overcome the barrier for the formation of a domain wall or of other configurations of magnetization reversal. There is some evidence that surface irregularities are responsible, at least in part, for the local variations of coercive force near the middle of the whisker in the experiment of DeBlois and Bean. Actually, when one of their samples was removed from its capillary to check its diameter under the microscope, then replaced and tested again, the first peak in coercive force was considerably reduced.[10] This might sound like a scratch on the surface rather than any damage to the internal structure. It should be noted, however, that the bucking field has been reduced in the meantime so that the first peak reduction might be due to inclusion of a larger part of the low coercive force material at the end. Also, DeBlois could not actually find a correlation between rough study of surface and local minima and maxima except in a few cases where surface imperfection was severe as were the local minima.[10] Anyhow, it does not seem reasonable that this alone can cause the discrepancy between theory and experiment, except probably for highly perfect crystals such as whiskers, since the discrepancy between theory and experiment is more severe for large samples than for small ones, while any surface effects are expected to be less important, the larger the crystal.

[1] W. F. Brown, Jr., J. Appl. Phys. **30**, 62S (1959).
[2] S. Shtrikman and D. Treves, J. phys. radium **20**, 286 (1959).
[3] A. Aharoni, J. Appl. Phys. **30**, 70S (1959).
[4] W. F. Brown, Jr., Revs. Modern Phys. **17**, 15 (1945).
[5] E. H. Frei, S. Shtrikman, and D. Treves, Phys. Rev. **106**, 446 (1957).
[6] R. W. DeBlois and C. P. Bean, Bull. Am. Phys. Soc. **3**, 267 (1958); J. Appl. Phys. **29**, 459 (1958); J. Appl. Phys. **30**, 225S (1959).
[7] A. Aharoni and S. Shtrikman, Phys. Rev. **109**, 1522 (1958).
[8] W. F. Brown, Jr., J. Appl. Phys. **29**, 470 (1958).
[9] W. F. Brown, Jr., Phys. Rev. **105**, 1479 (1957).
[10] R. W. DeBlois (private communication).

3. Crystal Imperfections

Crystal imperfections such as dislocations, impurities, cavities, etc., seem the most probable explanation for the success of the theory in the case of small particles and its failure in the case of large particles, since one would expect the probability of finding an imperfection to increase with particle size. Of the possible imperfections, the suggestion of Rathenau *et al.*[11] that domain walls might nucleate at regions where for some defect of structure the local anisotropy constant K is low, is adopted for the study reported in this paper. As a first approach extreme mathematical difficulties are avoided by treating only a one-dimensional model with only one region of imperfection.

More specifically, a ferromagnetic material infinite in all directions which has a uniaxial magnetocrystalline anisotropy $\bar{K}(x)$ is assumed. The external field H is applied along the z axis, which is assumed to coincide with the direction of easy magnetization. The easiest mode for magnetization changes is evidently rotation of the spins in the yz plane, so that the direction cosines are

$$\alpha_x=0, \quad \alpha_y=\sin\omega, \quad \alpha_z=\cos\omega, \tag{1}$$

where ω is assumed to be a function of x only.

Neglecting demagnetizing effects, the energy is

$$E=\int_0^\infty\left[A\left(\frac{d\omega}{dx}\right)^2+\bar{K}\sin^2\omega-HI_s\cos\omega\right]dx, \tag{2}$$

where A is the exchange constant, I_s the saturation magnetization. In writing (2) is was assumed that

$$\bar{K}(x)=\bar{K}(-x), \tag{3}$$

so that only $x\geqslant 0$ need be considered.

In a preliminary report[3] the nucleation field was given for the case

$$\begin{aligned}\bar{K}(x)&=0 \quad \text{for} \quad x\leqslant d,\\ &=K \quad \text{for} \quad x\geqslant d,\end{aligned} \tag{4}$$

and for the case

$$\begin{aligned}\bar{K}(x)&=Kx/d \quad \text{for} \quad x\leqslant d,\\ &=K \quad\quad \text{for} \quad x\geqslant d.\end{aligned} \tag{5}$$

In the following the complete study of the case expressed in (4) will be given.

II. THE NUCLEATION FIELD

The Euler differential equation, the solution of which is the minimum of the energy integral given by (2) is, when $\bar{K}$ is given by (4),

$$d^2\omega/dt^2-T^2h\sin\omega-\tfrac{1}{2}T^2\sin 2\omega=0, \quad t\geqslant 1, \tag{6a}$$

$$d^2\omega/dt^2-T^2h\sin\omega=0, \quad t\leqslant 1, \tag{6b}$$

where

$$t=x/d, \quad h=HI_s/2K, \quad T=dK^{\frac{1}{2}}A^{-\frac{1}{2}}, \tag{7}$$

ω and its derivative are continuous everywhere (in particular at $t=1$) and the boundary conditions are evidently

$$\omega'(0)=\omega'(\infty)=0. \tag{8}$$

It should be noted that h is defined in terms of $2K/I_s$, which is the coercive force for perfect material. Since the defined imperfection cannot make the magnetization reversal more difficult than when it is absent, the equations need be solved only for

$$|h|<1. \tag{9}$$

Starting as usual[5,9] with a material magnetized to saturation in the $+z$ direction and reducing the field, a value h_n is reached in which the saturation solution $\omega=0$ is no longer the stable solution of (6). Since any change starts by a *small* change, at nucleation one can write (6) in the form

$$d^2\omega/dt^2-T^2(1+h)\omega=0, \quad t\geqslant 1, \tag{10a}$$

$$d^2\omega/dt^2-T^2h\omega=0, \quad t\leqslant 1. \tag{10b}$$

It is readily seen that there is no continuous solution of (10) and (8) if $h\geqslant 0$, except for $\omega=0$. For $h<0$ only the region (9) is of interest and in it the only solution of (10) which fulfills (8) and is continuous at $t=1$ is

$$\begin{aligned}\omega&=C\exp[-T(1+h)^{\frac{1}{2}}(t-1)], \quad t\geqslant 1,\\ \omega&=C\cos[T(-h)^{\frac{1}{2}}t]/\cos[T(-h)^{\frac{1}{2}}], \quad t\leqslant 1.\end{aligned} \tag{11}$$

This function should also have a continuous derivative at $t=1$. This implies the following relation

$$-h_n=\cos^2 v_n, \tag{12a}$$

where

$$v=T(-h)^{\frac{1}{2}}. \tag{12b}$$

The solution of this transcendental equation is the required nucleation field. This field, calculated from (12), is plotted in Fig. 1 as a function of the reduced defect dimension T.

The question whether at nucleation the magnetization changes continuously or discontinuously is determined[5] by considering fourth order terms in ω

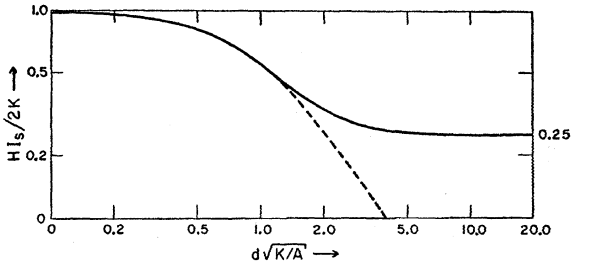

FIG. 1. The nucleation field (dashed) and coercive force (full curve) in terms of the coercive force of perfect material, $HI_s/2K$, as functions of the defect size, d.

[11] G. W. Rathenau, J. Smit, and A. L. Stuyts, Z. Physik **133**, 250 (1952).

in (2). This gives for the energy change at nucleation

$$\Delta E = B(v_n \tan v_n + 1 - 3\cos^2 v_n), \tag{13}$$

where B is a positive expression. Equation (13) yields a discontinuous jump of the magnetization at nucleation for $v_n < 0.732$ and a continuous change at nucleation for $v_n > 0.732$. Using (12) the region $0 < v_n < 0.732$ is equivalent to $0 < T < 0.984$.

III. SOLUTIONS OF THE DIFFERENTIAL EQUATION

At fields different from the nucleation field, the nonlinear equations (6) rather than (10) give the stationary states. In this part the mathematical solution only will be given and the physical significance will be discussed in part IV.

Equation (6b) is readily integrated and its general solution which fulfils $\omega'(0) = 0$ is

$$\omega = 2\arcsin[k\,\mathrm{sn}(u,k)], \quad t \leqslant 1, \tag{14a}$$

where

$$u = K(k) - T(-h)^{\frac{1}{2}}t, \tag{14b}$$

K is the complete elliptic integral of the first kind and sn is the amplitude sine[12] and k is to be regarded as an arbitrary constant. The envelope singular solutions

$$\omega = 0 \quad \text{and} \quad \omega = \pi \tag{15}$$

are also possible for any value of t.

Equation (6a) can be readily integrated once to yield

$$-\tfrac{1}{2}(d\omega/dt)^2 - T^2 h\cos\omega - \tfrac{1}{4}T^2\cos 2\omega = \tfrac{1}{2}A, \tag{16}$$

but further integration involves various types of functions depending on the value of the constant A, so that this constant needs to be evaluated first from the value of the function at infinity. Two branches need be considered.

1. $\omega(\infty) = 0$

Substituting this value and (8) in (16) one obtains

$$A = -T^2(2h + \tfrac{1}{2}),$$

and the general solution of (16), for the region (9), is

$$\omega = 2\arctan\frac{2C_1T(1+h)^{\frac{1}{2}}\exp[(1+h)^{\frac{1}{2}}Tt]}{1 - C_1^2T^2h\exp[2(1+h)^{\frac{1}{2}}Tt]}, \quad t \geqslant 1, \tag{17}$$

where C_1 is a constant (the only possible solution for $h \geqslant 1$ is (15), which is reasonable physically).

2. $\omega(\infty) = \pi$

Substituting this and (8) in (16) one obtains

$$A = -T^2(-2h + \tfrac{1}{2}),$$

and the general solution of (16) is

$$\omega = 2\arctan\frac{T^2h + C_2^2\exp[2(1-h)^{\frac{1}{2}}Tt]}{2T(1-h)^{\frac{1}{2}}C_2\exp[(1-h)^{\frac{1}{2}}Tt]}, \quad t \geqslant 1, \tag{18}$$

where C_2 is a constant.

In each case ω and $d\omega/dt$ should be continuous at $t = 1$. For case 2, using (18) and (14) this implies

$$2\arctan\frac{S_2^2 + T^2h}{2S_2T(1-h)^{\frac{1}{2}}} = 2\arcsin[k\,\mathrm{sn}(K - v, k)], \tag{19}$$

and

$$\frac{4T^2(1-h)S_2(S_2^2 - T^2h)}{S_2^4 + 2(2-h)T^2S_2^2 + T^4h^2} = -2T(-h)^{\frac{1}{2}}k\,\mathrm{cn}(K - v, k), \tag{20}$$

where v is given by (12b) and

$$S_2 = C_2\exp[T(1-h)^{\frac{1}{2}}]. \tag{21}$$

For $k\,\mathrm{sn}(K - v, k) = 1$ the only solution is $S_2 = 0$ which reduces (18) to the trivial solution (15). For $k\,\mathrm{sn}(K - v, k) \neq 1$ and for $h < 0$, one obtains by using the identity

$$\tan z = \sin z(1 - \sin^2 z)^{-\frac{1}{2}}, \tag{22}$$

in (19) and solving for S_2

$$S_2 = \frac{T(1-h)^{\frac{1}{2}}k\,\mathrm{sn}(K - v, k) + T[k^2\,\mathrm{sn}^2(K - v, k) - h]^{\frac{1}{2}}}{\mathrm{dn}(K - v, k)}. \tag{23}$$

Substituting this equation in (20)

$$vk\,\mathrm{cn}(K - v, k) + T[k^2\,\mathrm{sn}^2(K - v, k) - h]^{\frac{1}{2}}\,\mathrm{dn}(K - v, k) = 0. \tag{24}$$

Substituting the identities[13]

$$\mathrm{cn}(K - v, k) = \frac{k'\,\mathrm{sn}(v,k)}{\mathrm{dn}(v,k)},$$

$$\mathrm{sn}(K - v, k) = \frac{\mathrm{cn}(v,k)}{\mathrm{dn}(v,k)}, \tag{25}$$

$$\mathrm{dn}(K - v, k) = \frac{k'}{\mathrm{dn}(v,k)},$$

in (24) and rearranging, one obtains

$$k^2\,\mathrm{cn}^2(v,k) - h\,\mathrm{dn}^4(v,k) = 0. \tag{26}$$

Since $h < 0$ the two terms in (26) are non-negative and to be zero each should be zero which implies

$$k^2[1 - \mathrm{sn}^2(v,k)] = 1 - k^2\,\mathrm{sn}^2(v,k) = 0,$$

i.e.,

$$k^2 = \mathrm{sn}^2(v,k) = 1. \tag{27}$$

[12] P. F. Byrd and M. D. Friedman, *Handbook of Elliptic Integrals for Engineers and Physicists* (Springer-Verlag, Berlin, 1954).

[13] See reference 12, p. 20.

But for $k \to 1$ $\mathrm{sn}(v,k) \to \tanh v$ and can be 1 only for $v \to \infty$. It is therefore seen that (18) cannot be an analytic continuation of (14). On the other hand, if one tries $\omega'(1)=0$ in (18) the only possibility is $C_2=0$ which reduces (18) to (15). The solution (18) cannot therefore be an analytical continuation of (15) either, and the only possible solution for $t \geqslant 1$ is (15) or (17).

The continuity of (17) and (14) at $t=1$ implies relations similar to (19)–(20). Using again (22) and a procedure similar to the previous case, one ends in this case with the equation

$$-h=\mathrm{sn}^2(K-v,\, k)\ \mathrm{dn}^2(K-v,\, k),$$

or by using (25)

$$-h=(1-k^2)\ \mathrm{cn}^2(v,k)\ \mathrm{dn}^{-4}(v,k). \tag{28}$$

Substituting the value $k=0$ in (28) one obtains the nucleation field formula (12). Moreover, using the following approximations[14]

$$\mathrm{cn}(v,k) \approx \cos v + \tfrac{1}{4}k^2 \sin v(v - \sin v \cos v),$$
$$\mathrm{dn}(v,k) \approx 1 - \tfrac{1}{2}k^2 \sin^2 v,$$

which are valid for $k \ll 1$, in (28) it is found that for a constant T

$$(\partial k^2/\partial |h|)_{k=0} = C/(v_n \tan v_n + 1 - 3\cos^2 v_n), \tag{29}$$

where C is positive. This is the same expression as in (13), and actually if at nucleation $\partial k^2/\partial |h|$ is positive there is a continuous change and vice versa, as will be explained in part IV.

IV. THE COERCIVE FORCE

It has been shown that the only possible solutions are (15) and (17). Since before nucleation $\omega=0$, at nucleation the spins will follow the solution (17) if it is possible and if it is stable. Otherwise there will be a complete reversal to $\omega=\pi$. In order to follow (17) for a certain value of h and T there should be a value of k satisfying (28) and (12b). Supposing one plots the solutions of k as a function of h for a constant T. As long as $\partial k/\partial |h|$ is positive, increasing $|h|$ there is still a solution. However, when $k(|h|)$ starts to reverse, this can no longer be followed; and there is a jump either to the next branch on $k(h)$ curve if any, or to the solution $\omega=\pi$ if there are no more possible values of k for the larger $|h|$. In particular, at nucleation the solution of (28) is $k=0$ for any value of T. Therefore, there is a jump at nucleation if and only if $(\partial k/\partial |h|)_{k=0}$ is negative.

It is readily shown by integration that in the case (17), as well as for $\omega=0$, the average magnetization

$$j = \lim_{L\to\infty} \frac{1}{L} \int_0^L \cos\omega dx$$

is $+1$ (and its only other value is -1 for $\omega=\pi$). The magnetization curve is therefore rectangular with the coercive force identical with the value of h at which there is no longer any k satisfying (28).

The solutions of (28) were plotted, for various values of T, and it was found that in every case, there was only a single jump. In the region $T<0.984$, discussed in part II, the coercive force is identical with the nucleation field. For higher values of T the coercive force is larger than the nucleation, and its numerical results are plotted in Fig. 1 (full curve). The nucleation field is shown dotted on the same figure. It should be noted that while the nucleation field decreases considerably for large defect size T, the coercive force saturates very rapidly. In fact, it is always larger than $\frac{1}{4}$, as can be seen from the following argument.

It is very readily seen by plotting the elliptic integral of the first kind $F(k,\mu)$ that the equation

$$2kT = F(k,\mu) \tag{30a}$$

has a solution $k(<1)$ *for every value of* T and for

$$\mu = \arcsin[(2k^2-1)^{\frac{1}{2}}/k]. \tag{30b}$$

Equations (30) can be joined to read

$$\mathrm{sn}(2kT,k) = (2k^2-1)^{\frac{1}{2}}/k. \tag{31}$$

Using these values of k and T in (28) and (12b) one gets the solution

$$|h| = (4k^2)^{-1}. \tag{32}$$

It is therefore shown that for every value of T, there is a solution k of (28) and (12b) for the field $(4k^2)^{-1}$ and therefore a solution for the field $\frac{1}{4}$, since $k^2 \leqslant 1$. Since the coercive force has been shown to be the value of h from which there is no solution k, this is certainly larger than $\frac{1}{4}$.

V. DISCUSSION

The results given in Fig. 1 are not so encouraging as they seemed when only the preliminary results were known in the former report.[3] The fact that the reduction in the coercive force is never by more than a factor of 4 with respect to the perfect material cannot explain the experimentally observed reduction of some orders of magnitudes. It should be noted however that a reduction of $\frac{1}{2}$ is obtained for a rather small dimension of the imperfection. This is especially noted for materials which have high magnetocrystalline anisotropy, like MnBi. Taking for this material $A \approx 10^{-6}$ erg/cm and $K=10^7$ erg/cm^3 one obtains that the reduction of the coercive force to $\frac{1}{2}$ at $T=1$ is for a defect 30 A wide. This might suggest that dislocations may reduce the coercive force, provided a further study will show that a number of small defects of the same type can reduce the coercive force much more than the reduction to $\frac{1}{4}$ which is the maximum for *one* imperfection of any

[14] See reference 12, Eq. (127.01).

dimension. It might also be possible to obtain larger reductions for slow local decrease in K instead of the step-function (4).

At nucleation something similar to a domain wall is found in the case studied but this has not freedom of movement and therefore does not change the magnetization. It seems that in the case (5) a wall nucleated might move more easily, but in that case the nucleation field is[3] rather large for reasonable defect dimensions. A combination of (4) and (5) might therefore give an easy nucleation of movable wall and therefore a much higher decrease in the coercive force.

PHYSICAL REVIEW VOLUME 119, NUMBER 1 JULY 1, 1960

Etch Pits on Dendritic Germanium. A Clarification

P. J. HOLMES
Research Laboratory, Associated Electrical Industries, Aldermaston Court, Aldermaston, Berkshire, England
(Received February 1, 1960)

Previous reports by Billig and Holmes of the orientations of etch pits on the main faces of germanium dendrites are not at first sight consistent with those recently reported by Bennett and Longini. It is shown that this discrepancy arose because the orientation of equilateral pits on {111} surfaces depends on the etchant used. A check on the earlier work confirms that there is in fact no contradiction: ferricyanide and WAg etches produce pits which point upwards on "perfect" faces grown in a "G direction," while superoxol and similar etchants give pits pointing downwards.

A RECENT publication by Bennett and Longini[1] has brought to light some confusion, concerning the directions in which triangular pits point on etched dendritic germanium, in the reports originally published from this Laboratory.[2,3] These contained an error which is attributable to the fact that, at the time, it was not appreciated that the direction is also dependent on the actual etchant employed. On {111} surfaces, the WAg and ferricyanide etches form equilateral pits which appear, in plan, as if they were bounded by facets of {111} form, although they are actually much shallower.[4] The No. 2 (Superoxol) etch, and others with the same components, give equilateral pits which resemble, in plan, {100} facets. The edges of these two types of pit are both $\langle 1\bar{1}0\rangle$ lines, but their apices point in opposite directions (Fig. 1).

The structure diagram in reference 2 (p. 357) does, in fact, show clearly what the orientation of "{111}" type pits should be on the "perfect" and "imperfect" faces: they should always point upwards and downwards, respectively. The directions illustrated are, however, correct for "{100}" type pits. Likewise in reference 3, the drawings of x-ray diffraction patterns are correct for the faces illustrated (one {111} point would be $70\frac{1}{2}°$ above the center on the "perfect" face, indicating an upwards tilt of this plane), but the etch pit directions shown are only correct for "{100}" pits. The results of Bennett and Longini, whose dendrites contain an odd number of twin planes and therefore have two faces grown in the orientation corresponding to our "perfect" faces, are thus in accordance with this scheme: the WAg etch gives pits pointing upwards on both sides of the specimen.

Our use of the term "imperfect" to describe the development of faces of the opposite orientation is a relative one, and careful reading of reference 2 reveals no mention of asterism in x-ray photographs, which were all taken by the present author; no distortion of the

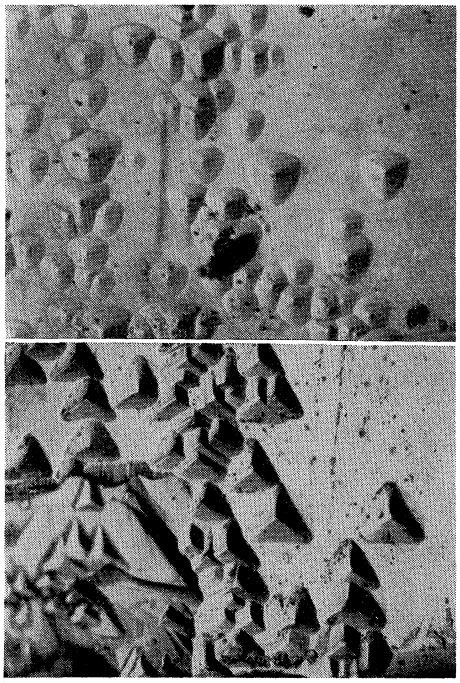

(a)

(b)

FIG. 1. (a) (above) Ge dendrite, "perfect" face, etched with 1 HF:1 H_2O_2:64 H_2O for 10 min. (b) (below) Same area, re-etched with ferricyanide etch for $1\frac{1}{2}$ min. (×280).

[1] A. I. Bennett and R. L. Longini, Phys. Rev. **116**, 53 (1959).
[2] E. Billig, Proc. Roy. Soc. (London) **A229**, 346 (1955).
[3] E. Billig and P. J. Holmes, Acta Cryst. **8**, 353 (1955).
[4] P. J. Holmes, Acta Met. **7**, 283 (1959).